

eeMC: Comments on Asymmetries in QED

Ian M. Nugent*
Victoria, B.C., Canada

Abstract

In the Quantum Electrodynamics process $e^+e^- \rightarrow l^+l^-(n\gamma)$, there are two well known angular asymmetries in the $\cos(\theta)$ and the $\cos(\theta^*)$ distributions. In this paper, the QED angular asymmetry related to the $\cos(\theta^*)$ distribution is investigated in terms of the Dirac propagator and the associated boundary conditions from which the Dirac propagator is constructed and the potential implications are examined.

Keywords: Electron-Positron Collider, Tau Lepton, Monte-Carlo Simulation

1 Introduction

In Quantum Electrodynamics (QED) processes, the higher order emission of hard photons directly influences the angular dependence in the differential cross-section. Consequently, for the $e^+e^- \rightarrow \mu^+\mu^-(\gamma)$ and $e^+e^- \rightarrow \tau^+\tau^-(\gamma)$ processes, this is related to the angular asymmetry between the outgoing charged leptons $\cos(\theta)$ [1, 2, 3, 4, 5, 6, 7] and $\cos(\theta^*)$ [8], asymmetry in the angle between the outgoing lepton and the radiated hard photon in the center-of-mass frame of the outgoing lepton pair. Higher order contributions, in particular, Feynman Diagrams with $k=2, \dots$ internal photon exchanges further modify the $\cos(\theta)$ asymmetry [9]¹, where the virtual and soft-photon contributions are most significant. This is in contrast to the $\cos(\theta^*)$ angular distributions, where the asymmetry originates from the inclusion of Feynman Diagrams that contain $n=1$ or more real hard photon emissions. In *eeMC* [10], each of the hard matrix elements, \mathcal{M}_n^k for n real hard photon emissions and k internal photon exchanges, are explicitly calculated without approximations from the Gamma-Matrices and Dirac spinors using an object-oriented structure. This allows for the investigation of the angular asymmetry $\cos(\theta^*)$ in terms of the treatment of the Dirac propagator and the associated boundary conditions.

2 Overview of eeMC Formalism

The *eeMC* [10] Monte-Carlo generator, is a stand-alone software program which contains the random-number generation [11, 12, 13, 14, 15], the phase-space generation [10, 16] based on the [17] algorithm modified to include embedded importance sampling [18, 19] and the theoretical models for the QED processes $e^-e^+ \rightarrow \mu^+\mu^-(n\gamma)$, $e^-e^+ \rightarrow \tau^+\tau^-(n\gamma)$, $e^-e^+ \rightarrow \text{hadrons}(n\gamma)$ and τ lepton decays. The cross-section for the QED processes $e^-e^+ \rightarrow \mu^+\mu^-(n\gamma)$, $e^-e^+ \rightarrow \tau^+\tau^-(n\gamma)$ and $e^-e^+ \rightarrow \text{hadrons}(n\gamma)$ is

constructed within the Yennie-Frautschi-Suura (YFS) Exponentiation Formalism [20] for the infra-red subtraction

$$d\sigma = \frac{\sum_{n=0}^{\infty} \prod_{i=0}^n \prod_{j=0}^i F(Y_{i,j}^{O(\alpha)}(P_i^\mu, P_j^\mu)) |\sum_{k=1}^{\infty} \bar{\mathcal{M}}_n^k|^2 dPS_n}{4(|\vec{P}_{e^-} - E_{e^+} + E_{e^-} - |\vec{P}_{e^+}|)} \quad (1)$$

where $F(x)$ is some functional form representing the resummation of all permutations for soft or virtual photon exchanges. For the Initial and Final YFS multiplicative subtraction, the function form $F(x)$ is the standard exponential YSF Form-Factor for the Yennie-Frautschi-Suura calculation [20]; the KK2F approximation [21]; and the Sudakov Form-Factor [3]. For the Full LO calculation from [22] applying corrections from [3, 10, 23], the $F(x)$ is the product of the exponential Form-Factor determined from [22] with the Coulomb potential factored out into a separate multiplicative resummation series, the Sommerfeld-Sakharov resummation factor [23]. The hard matrix elements, $\bar{\mathcal{M}}_n^k$, is determined with the spin-average-sum for an arbitrary Initial-State spin configuration [24] and is explicitly determined from the Feynman calculus corresponding to each Feynman Diagrams using an object-orientated representation of the Gamma-Matrices and Dirac Spinors [10]. Ward's Identity [6] is applied to incorporate the renormalization through the running of electromagnetic coupling constant [10, 25, 26]. Details on the simulation of the τ decays can be found in [10, 27].

3 Dirac Propagator Formalism

It is well known that the Dirac propagator can be described in terms of the retarded Green's function for a free particle with retarded boundary conditions [3],

$$G = i < 0 | \{ \psi_a(x') \bar{\psi}_b(x) \} | 0 > \theta(x'_{(0)} - x_{(0)}). \quad (2)$$

From which it follows that:

$$\left(\gamma^\mu \frac{\partial}{\partial x^\mu} - m \right) G(x' - x) = \delta^4(x' - x). \quad (3)$$

*Corresponding Author

Email: inugent.physics@outlook.com

¹These are the most significant terms in the infinite perturbative series.

Using the Fourier Transform between the momentum and the coordinate space[2, 3, 4], this can trivially be represented as:

$$G(p) = \frac{1}{\not{p}-m} = \frac{\not{p}+m}{p^2-m^2} \quad (4)$$

[2, 3, 4]. It is the retarded Green's function, Equation 4, which is generally used to describe the propagator for each internal fermion line in perturbation theory [2, 3, 4, 5, 6, 7]. In contrast, the Dirac propagator defined with the Feynman Boundary conditions is written as:

$$\begin{aligned} G(x'-x) &= \int \frac{d^4p}{(2\pi)^4} e^{-ip \cdot (x'-x)} G(p) \\ &= -i \int \frac{d^4p e^{ip \cdot (x'-x)}}{(2\pi)^3 2E} \left((\gamma^0 E - \boldsymbol{\gamma} \cdot \mathbf{p} + m) e^{-iE(t'-t)} \theta(t'-t) \right. \\ &\quad \left. + (-\gamma^0 E - \boldsymbol{\gamma} \cdot \mathbf{p} + m) e^{-iE(t-t')} \theta(t-t') \right) \\ &= -i \int \frac{d^3p}{(2\pi)^3 2E} \left(\sum_s u_a^s(p) \bar{u}_b^s e^{-ip \cdot (x'-x)} \theta(t'-t) \right. \\ &\quad \left. - \sum_s v_a^s(p) \bar{v}_b^s e^{-ip \cdot (x-x')} \theta(t-t') \right) \\ &= -i \int \frac{d^3p}{(2\pi)^3} \left(\frac{m}{E} \Lambda_+ e^{-ip \cdot (x'-x)} \theta(t'-t) \right. \\ &\quad \left. + \frac{m}{E} \Lambda_- e^{-ip \cdot (x-x')} \theta(t-t') \right) \\ &= -i < 0 | T \{ \psi_a(x') \bar{\psi}_b(x) \} | 0 >. \end{aligned} \quad (5)$$

[2, 3] Λ_+ and Λ_- are the standard positive and negative projection operators for the Dirac spinors,

$$\Lambda_+ = \frac{(\not{p}+m)}{2m}, \quad \Lambda_- = \frac{(-\not{p}+m)}{2m} \quad (6)$$

[2]. This is a time-ordered solution, where the integration contour for $t'-t > 0$ is in the lower half of the plane and corresponds to the positive energy solution while the integration contour for $t'-t < 0$ is in the upper half plane and corresponds to the negative energy solution. The $\not{p}-m$ and $\not{p}+m$ factors project out the positive and negative contribution to the propagator. Then, given that $(\sum_s u_a^s(p) \bar{u}_b^s = (\not{p}+m)$ and $\sum_s v_a^s(p) \bar{v}_b^s = (-\not{p}+m)$, and Equation 5 it follows that $G_+ = \frac{\not{p}+m}{p^2-m^2}$ and $G_- = \frac{-\not{p}+m}{p^2-m^2}$ for the positive and negative energy states going forward and backward in time respectively. From the derivation of the Feynman calculus, it can be seen that before applying Wick's Theorem to obtain the non-vanishing propagators and vertices, the expectation values in the s -matrix for the perturbative expansion must be time-ordered [2]. Naively, this implies that the Dirac propagators should also be time-ordered. Therefore, if one applies the Green's function with Feynman boundary conditions directly to the positive energy fermion states ($u^s(p)$) and negative energy fermion states ($v^s(p)$), taking into account the time-ordered direction of the particle/anti-particle states one obtains interesting results in terms of the angular asymmetries in QED²³. Fig-

²At this stage we would like to remind the reader of the Feynman rules for writing down the fermion line in the QED process $f^+ f^- \rightarrow f'^+ f'^-$. More specifically, going right to left for incoming particles, one starts with the positive energy state going forward in time to the electro-magnetic vertex and then proceeds backwards in time for the anti-fermion line. Similarly, for the outgoing particles one starts with the anti-fermion line going backwards in time to the QED vertex, and then proceeds forward in time for the outgoing fermion line.

³This formulation of the Dirac propagator also has implications for the box-diagram terms. We noted that in other processes, for example the $K_L K_S$ mass difference [2], that Feynman boundary conditions for the Dirac propagator are consistent with known results.

ure 1 presents radiative Born plus LO cross-section dependence on the angle between the emitted γ and the outgoing lepton (μ^- or τ^-) in the center-of-mass frame for the outgoing lepton-pair, $\cos(\theta^*)$. The reported asymmetry in the $\cos(\theta^*)$ distribution [8, 28], is reproduced by the Dirac propagator corresponding to the retarded Green's function solution. The asymmetry is most significant at $\cos(\theta^*) = \pm 1$. This region is removed in many other MC generators. The $\cos(\theta^*)$ angular asymmetry is more strongly peaked in the $e^+ e^- \rightarrow \mu^+ \mu^- (\gamma)$ process while the $e^+ e^- \rightarrow \tau^+ \tau^- (\gamma)$ process is more spread out, a consequence of the larger τ mass. When the time-ordered propagator is applied for the corresponding particle and anti-particle respectively, no asymmetry is observed in the $\cos(\theta^*)$ distribution. This suggests that the $\cos(\theta^*)$ asymmetry in QED is directly related to the choice of the Dirac propagator and the application in the perturbation theory.

4 Conclusion

The $\cos(\theta^*)$ asymmetries in the $e^+ e^- \rightarrow \mu^+ \mu^- (\gamma)$ and $e^+ e^- \rightarrow \tau^+ \tau^- (\gamma)$ QED interactions were investigated in terms of the choice of boundary conditions applied in the formulation of the Dirac propagators. The differential cross-section is symmetric in $\cos(\theta^*)$ for the Feynman boundary conditions which incorporate the time-ordering of the positive and negative energy Dirac states when applied to the Born and LO simulation, while the retarded Green's function for the Dirac propagator has a clear asymmetry. The asymmetry is most significant at $\cos(\theta^*) = \pm 1$, where due to the mass of the τ lepton is more visible away from the angular boundaries for the $e^+ e^- \rightarrow \tau^+ \tau^- (\gamma)$. We argue that applying the Feynman boundary conditions for the Dirac propagator is more consistent with the time-ordering from which the perturbative s -matrix is constructed.

Acknowledgement

GCC Version 4.8.5 was used for compilation and the plots are generated using the external program GNUPlot [29].

References

- [1] ALEPH Collaboration, DELPHI Collaboration, L3 Collaboration, OPAL Collaboration, SLD Collaboration, LEP Electroweak Working Group, SLD Electroweak, Heavy Flavour Groups. Precision Electroweak Measurements on the Z Resonance. *Physics Reports*, 427(5):257-454, 2006. doi: 10.1016/j.physrep.2005.12.006.
- [2] P. Renton. *Electroweak Interactions: An Introduction to the Physics of Quarks and Leptons*. Cambridge University Press, New York, USA, 5 1990. ISBN 978-0-521-36692-2.
- [3] Michael E. Peskin and Daniel V. Schroeder. *An Introduction to Quantum Field Theory*. Addison-Wesley, Reading, USA, 1995. ISBN 978-0-201-50397-5.
- [4] F. Halzen and Alan D. Martin. *Quarks And Leptons: An Introductory Course In Modern Particle Physics*. John Wiley & Sons, USA, 1 1984. ISBN 978-0-471-88741-6.
- [5] L.H. Ryder. *Quantum Field Theory*. Cambridge University Press, New York, USA, 6 1996. ISBN 978-0-521-47814-4, 978-1-139-63239-3, 978-0-521-23764-2.
- [6] Franz Mandl and Graham Shaw. *Quantum Field Theory: Revised Edition*. John Wiley & Sons, Great Britain, 1 1985.

- [7] David J. Griffiths. *Introduction to Elementary Particle*. John Wiley & Sons, USA, 1987.
- [8] J.P. Lees et al. Measurement of Initial-State/Final-State Radiation Interference in the Processes $e^+e^-\mu^+\mu^-\gamma$ and $e^+e^-\pi^+\pi^-\gamma$. *Phys. Rev. D*, 92:072015, 2015. doi: 10.1103/PhysRevD.92.072015.
- [9] F. Campanario, H. Czyż, J. Gluza, M. Gunia, T. Riemann, G. Rodrigo, and V. Yundin. Complete QED NLO Contributions to the Reaction $e^+e^-\rightarrow\mu^+\mu^-\gamma$ and Their Implementation in the Event Generator PHOKHARA. *JHEP*, 02:114, 2014. doi: 10.1007/JHEP02(2014)114.
- [10] I. M. Nugent. **eeMC**: Simulation of $e^+e^-\rightarrow\mu^+\mu^-(\gamma)$ and $e^+e^-\rightarrow\tau^+\tau^-(\gamma)$ Events. 2022. arXiv: 2202.02318 [hep-ph].
- [11] M. Matsumoto and T. Nishimura. Mersenne Twister: a 623-Dimensionally Equidistributed Uniform Pseudo-Random Number Generator. *ACM Trans. Model. Comput. Simul.*, 8:3–30, 1998. doi: 10.1145/272991.272995.
- [12] T. Nishimura. Tables of 64-bit Mersenne twisters. *ACM Trans. Model. Comput. Simul.*, 10:348–357, 2000. doi: 10.1145/369534.369540.
- [13] S. Harase and T. Kimoto. Implementing 64-bit Maximally Equidistributed F2-Linear Generators with Mersenne Prime Period. *ACM Trans. on Mathematical Software*, 44:1–11, 2018. doi: 10.1145/3159444.
- [14] S. Vigna. An Experimental Exploration of Marsaglia’s xorshift Generators, Scrambled. 2016. arXiv: 1402.6246.
- [15] D. E. Knuth. *The Art of Computer Programming Vol 2 (2nd Ed.)*. Addison-Wesley, Reading, USA, 1981.
- [16] I. M. Nugent. **eeMC**: Higher Order Radiative Emissions for $e^+e^-\rightarrow\mu^+\mu^-(n\gamma)$ and $e^+e^-\rightarrow\tau^+\tau^-(n\gamma)$ Events. 2022. arXiv: 2212.05388 [hep-ph].
- [17] E. Byckling and K. Kajantie. n-Particle Phase Space in Terms of Invariant Momentum Transfer. *Nucl. Phys. B*, 9:568–576, 1969. doi: 10.1016/0550-3213(69)90271-5.
- [18] Dani Gamerman and Hedibert F. Lopes. *Markov Chain Monte Carlo: Stochastic Simulation for Bayesian Inference 2nd ed.* Chapman & Hall/CRC Taylor & Francis Group, 2006.
- [19] Andrew Gelman, John B. Carlin, Hal S. Stern, David B. Dunson, Aki Vehtari, and Donald B. Rubin. *Bayesian Data Analysis 3rd Ed.* CRC Press Taylor & Francis Group, 2014.
- [20] D. R. Yennie, S. C. Frautschi, and H. Suura. The Infrared Divergence Phenomena and High-Energy Processes. *Annals of Physics*, 13:379–452, 1961. doi: 10.1016/0003-4916(61)90151-8.
- [21] S. Jadach, B.F.L. Ward, and Z. Wąs. The Precision Monte Carlo Event Generator KK For Two-Fermion Final States In e^+e^- Collisions. *Comput. Phys. Commun.*, 130:260–325, 2000. doi: 10.1016/S0010-4655(00)00048-5.
- [22] J. Schwinger. *Particle, Sources, and Fields Volumes I-III*. Perseus Books Publishing, L.L.C., Reading, Massachusetts, USA, 1998.
- [23] B. Smith and M.B. Voloshin. $e^+e^-\rightarrow\tau^+\tau^-$ at Threshold and Beyond. *Phys. Lett. B*, 324(1):117–120, 1994. doi: 10.1016/0370-2693(94)00095-6.
- [24] I. M. Nugent. **eeMC**: Arbitrary Initial Spin States for the Production of $e^+e^-\rightarrow\mu^+\mu^-(\gamma)$ and $e^+e^-\rightarrow\tau^+\tau^-(\gamma)$ Events. 2022. arXiv: 2202.02318 [hep-ph].
- [25] Friedrich Jegerlehner. *The Anomalous Magnetic Moment of the Muon*. Springer Tracts in Modern Physics 226, Heidelberg, Germany, 2007.
- [26] Christian Sturm. Leptonic Contributions to the Effective Electromagnetic Coupling at Four-Loop Order in QED. *Nuclear Physics B*, 874(3):698–719, Sep 2013. ISSN 0550-3213. doi: 10.1016/j.nuclphysb.2013.06.009.
- [27] I. M. Nugent. **eeMC**: Low energy Mesons and the residual QCD Potential. 2023. arXiv: 2312.01470 [hep-ph].
- [28] S. Actis et al. Quest for Precision in Hadronic Cross-Sections at Low Energy: Monte Carlo Tools vs. experimental Data. *The European Physical Journal C*, 66(3-4):585–686, 2010. doi: 10.1140/epjc/s10052-010-1251-4.
- [29] Thomas Williams, Colin Kelley, et al. Gnuplot 4.2: An Interactive Plotting Program. <http://gnuplot.sourceforge.net/>, 2007.

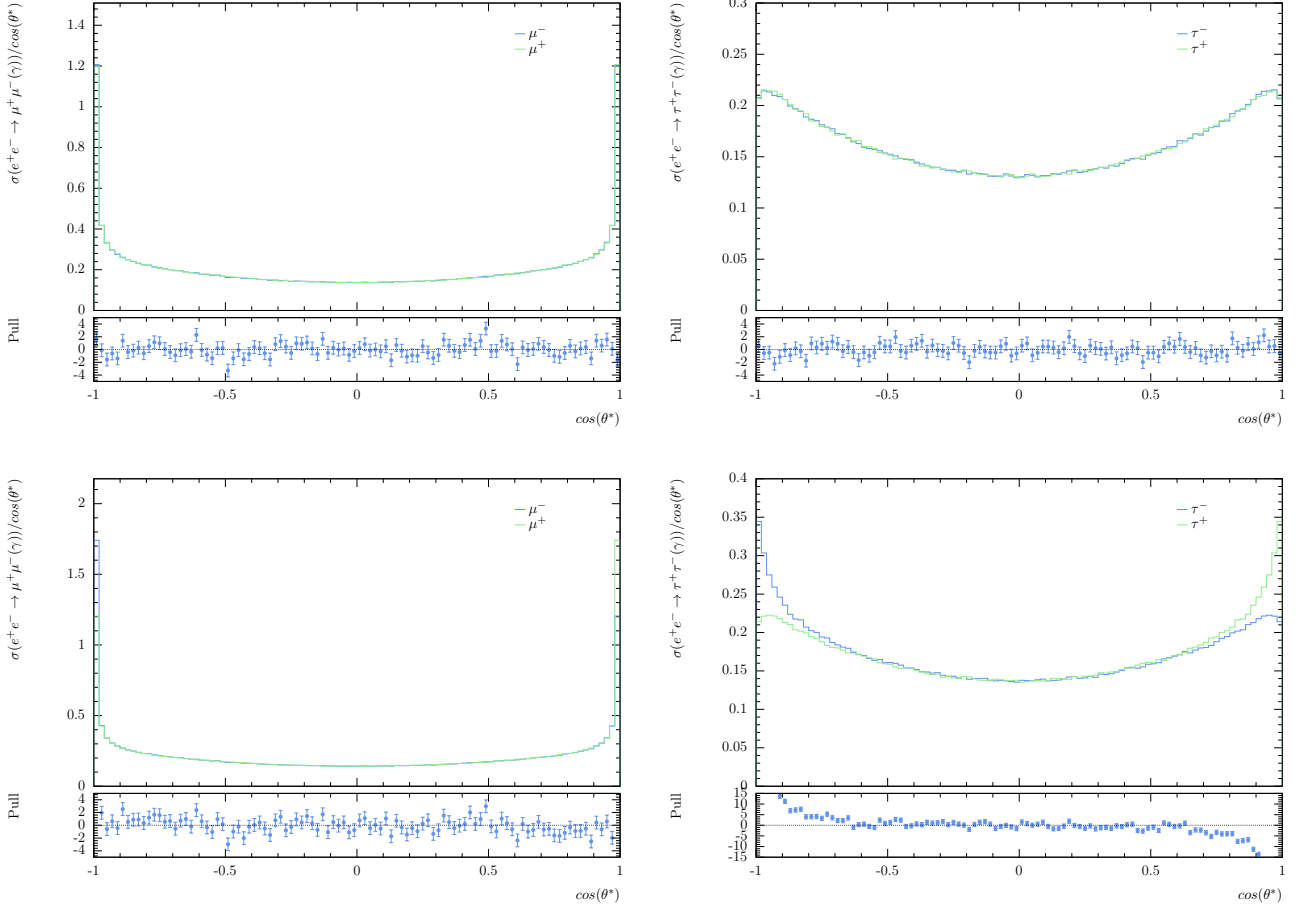


Figure 1: The $\cos(\theta^*)$ distribution for Born+LO determined with the Dirac propagator constructed from the Feynman boundary conditions (top) and the retarded Dirac propagator (bottom) for the $e^+e^- \rightarrow \mu^+\mu^-(\gamma)$ (left) and $e^+e^- \rightarrow \tau^+\tau^-(\gamma)$ (right) QED interactions for a center-of-mass energy of $10.58 GeV/c^2$ and a soft-photon cut-off of $E_l=1 MeV$. The blue line represents the $\cos(\theta^*)$ angle between the photon and l^- in the rest frame of the outgoing lepton pair, while the green line represents the $\cos(\theta^*)$ angle between the photon and l^+ in the rest frame of the outgoing lepton pair.